Chapter 1

Fundamentals of NMR

THOMAS L. JAMES

Department of Pharmaceutical Chemistry

University of California

San Francisco, CA 94143-0446 U.S.A.

SUMMARY

   The general phenomenon of nuclear magnetic resonance is introduced using both a classical and a quantum mechanical perspective. This provides the basis for understanding measurable and informative NMR parameters: chemical shift, spin-spin splitting, linewidths, relaxation, the nuclear Overhauser effect and chemical exchange. The emphasis here is on molecules in solution but much of the fundamentals pertain to molecules in the gas or solid phase as well.

1.1 Introduction

From a purely intellectual viewpoint, one of the fascinating things about nuclear magnetic resonance (NMR) is the complexity of the subject. However, this complexity can be the source of much frustration for those wishing to understand and use NMR. As with other physical techniques used in studies of biological systems, NMR may be used in an empirical mode; for example, simply noting variations in an NMR parameter with alteration of an experimental variable. However, a better understanding of the NMR phenomenon is often rewarded with additional elucidation of the system under study. Although there may be thresholds of knowledge of NMR necessary to read the literature critically or to conduct NMR studies, there is a continuum of knowledge to be gained about NMR that has the practical dividend of enabling an ever greater variety of NMR experiments to be utilized correctly. This chapter is intended to provide an introduction to the NMR phenomenon. A more thorough coverage of the principles can be found in the rigorous (mathematically oriented) texts of Abragam (Abragam, 1961) and Ernst *et al* (Ernst et al., 1987) A good introductory text was written by Derome (Derome, 1987) With an orientation primarily towards protein structure determination, a good description of background and applications is found in the monograph of Cavanagh *et al* (Cavanagh et al., 1996). Other recent volumes contain chapters describing both principles and applications, with an eye towards investigation of proteins and nucleic acids James and Oppenheimer, 1994; James, 1995; Reid, 1997.

The nuclear magnetic resonance phenomenon can be described in a nutshell as follows. If a sample is placed in a magnetic field and is subjected to radiofrequency (RF) radiation (energy) at the appropriate frequency, nuclei in the sample can absorb the energy. The frequency of the radiation necessary for absorption of energy depends on three things. First, it is characteristic of the type of nucleus (e.g., ^{1}H or ^{13}C). Second, the frequency depends on chemical environment of the nucleus. For example, the methyl and hydroxyl protons of methanol absorb at different frequencies, and amide protons of two different tryptophan residues in a native protein absorb at different frequencies since they are in different chemical environments. The NMR frequency also depends on spatial location in the magnetic field if that field is not everywhere uniform. This last variable provides the basis for magnetic resonance imaging (MRI), for self-diffusion coefficient measurements, and for coherence selection – topics which will not be discussed further in this introductory chapter. For diffusion coefficient measurements and for imaging, the magnetic field is made to vary linearly over the sample. However, for most spectroscopic purposes we generally wish the magnetic field to be as homogeneous as possible over the sample. The homogeneity requirements for NMR spectroscopy are rather stringent; the magnetic field should vary no more

2

than 10 parts per billion (ppb) over the sample volume. After absorption of energy by the nuclei, the length of time and the manner in which the nuclei dissipate that energy can also be used to reveal information regarding a variety of dynamic processes.

1.2 Magnetic Resonance
1.2.1 Nuclear spins

Nuclei have positive charges. Many nuclei behave as though they were spinning. Anything that is charged and moves has a magnetic moment and produces a magnetic field. Therefore, a spinning nucleus acts as a tiny bar magnet oriented along the spin rotation axis (Figure 1.1). This tiny magnet is often called a nuclear spin. If we put this small magnet in the field of a much larger magnet, its orientation will no longer be random. There will be one most probable orientation. However, if the tiny magnet is oriented *precisely* 180° in the opposite direction, that position could also be maintained (play with a couple magnets to test this). In scientific jargon the most favorable orientation would be the low-energy state and the less favorable orientation the high-energy state.
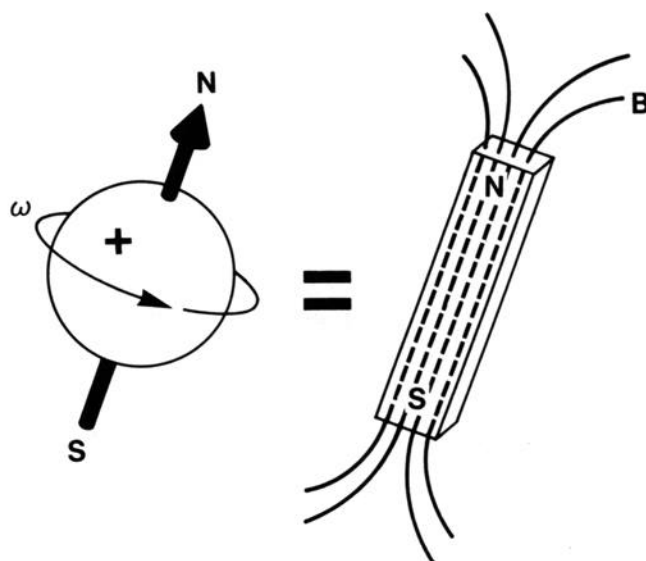
_____

Figure 1.1: The charged nucleus (e.g., ^{1}H) rotating with angular frequency   ($= 2$) creates a magnetic field B and is equivalent to a small bar magnet whose axis is coincident with the spin rotation axis.

_____

This two-state description is appropriate for most nuclei of biologic interest including ^{1}H, ^{13}C, ^{15}N, ^{19}F, and ^{31}P; i.e., all those which have nuclear spin quantum number I = l/2. It is a quantum mechanical requirement that any individual nuclear spins of a nucleus with I = l/2 be in one of the two states (and nothing in between) whenever the nuclei are in a magnetic field. It is important to note that the most common isotopes of carbon, nitrogen and oxygen (^{12}C, ^{14}N and ^{16}O) do not have a nuclear spin.

1.2.2 The Resonance Phenomenon

  The small nuclear magnet may spontaneously "flip" from one orientation (energy state) to the other as the nucleus sits in the large magnetic field. This relatively infrequent event is illustrated at the left of Figure 1.2. However, if energy equal to the difference in energies (ΔE) of the two nuclear spin orientations is applied to the nucleus (or more realistically, group of nuclei), much more flipping between energy levels is induced (Figure 1.2). The irradiation energy is in the RF range (just like on your FM radio station) and is typically applied as a short (e.g., many microseconds) pulse. The absorption of energy by the nuclear spins causes transitions from higher to lower energy as well as from lower to higher energy. This two-way flipping is a hallmark of the resonance process. The energy absorbed by the nuclear spins induces a voltage that can be detected by a suitably tuned coil of wire, amplified, and the signal displayed as a *free induction decay (FID).* Relaxation processes *(vide infra)* eventually return the spin system to thermal equilibrium, which occurs in the absence of any further perturbing RF pulses.
  The energy required to induce flipping and obtain an NMR signal is just the energy difference between the two nuclear orientations and is shown in Figure 1.3 to depend on the strength of the magnetic field B_o in which the nucleus is placed:

$$\Delta E = \gamma h B_o / 2\pi \qquad\qquad\qquad [1.1]$$

where h is Planck's constant (6.63 x 10^{-27} erg sec). The Bohr condition ($\Delta E = h\nu$) enables the frequency ν_o of the nuclear transition to be written as

$$\nu_o = \gamma B_o / 2\pi \qquad\qquad\qquad [1.2]$$

Equation 1.2 is often referred to as the Larmor equation, and $\omega_o = 2\pi\nu_o$ is the angular *Larmor resonance frequency*. The *gyromagnetic ratio* γ is a constant for any particular type of nucleus and is directly proportional to the strength of the tiny nuclear magnet. Table 1.1 lists the gyromagnetic ratios for several nuclei of biologic interest. At magnetic field strengths used in NMR experiments the frequencies
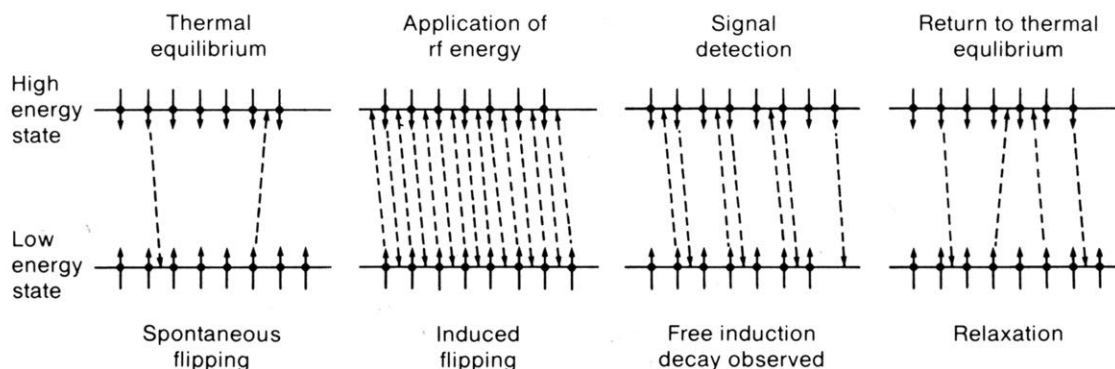
4

Figure 1.2: For nuclei (I=1/2) in a magnetic field of strength B_o at thermal equilibrium, i.e.,

unperturbed, there will be infrequent flips of individual nuclear spins between the two different energy

levels. When a radiofrequency (RF) pulse with appropriate energy is applied (i.e., equal to the difference

in energies of the two levels), transitions between the two energy levels will be induced, i.e., the nuclear

spin system will "resonate"; the spin system absorbs the energy. Following the RF pulse, a signal termed

a free induction decay or FID can be detected as a result of the voltage induced in the sample by the

energy absorption. Eventually the nuclear spin system relaxes to the thermal equilibrium situation.

necessary to fulfill the resonance condition (Equation 1.2) are in the RF range; e.g. in a magnetic field of

14.1 T the transition frequency $_o$ for ^{1}H is 600 MHz, for ^{15}N is 60.8 MHz and for ^{13}C is 151 MHz.

1.2.3 Sensitivity and the Boltzmann Equation

We noted earlier that our small bar magnet (nuclear spin) could be oriented in one of two ways.

The extent to which one orientation (energy state) is favored over the other depends on the strength

of the small nuclear magnet (proportional to gyromagnetic ratio) and the strength of the strong

magnetic field B_o in which it is placed. In practice, we do not put one nucleus in a magnetic field.

Rather a huge number (approaching Avogadro's number) of nuclei are in the sample that is placed

in a magnetic field. The distribution of nuclei in the different energy states (i.e., orientations of

nuclear magnets) under conditions in which the nuclear spin system is unperturbed by application
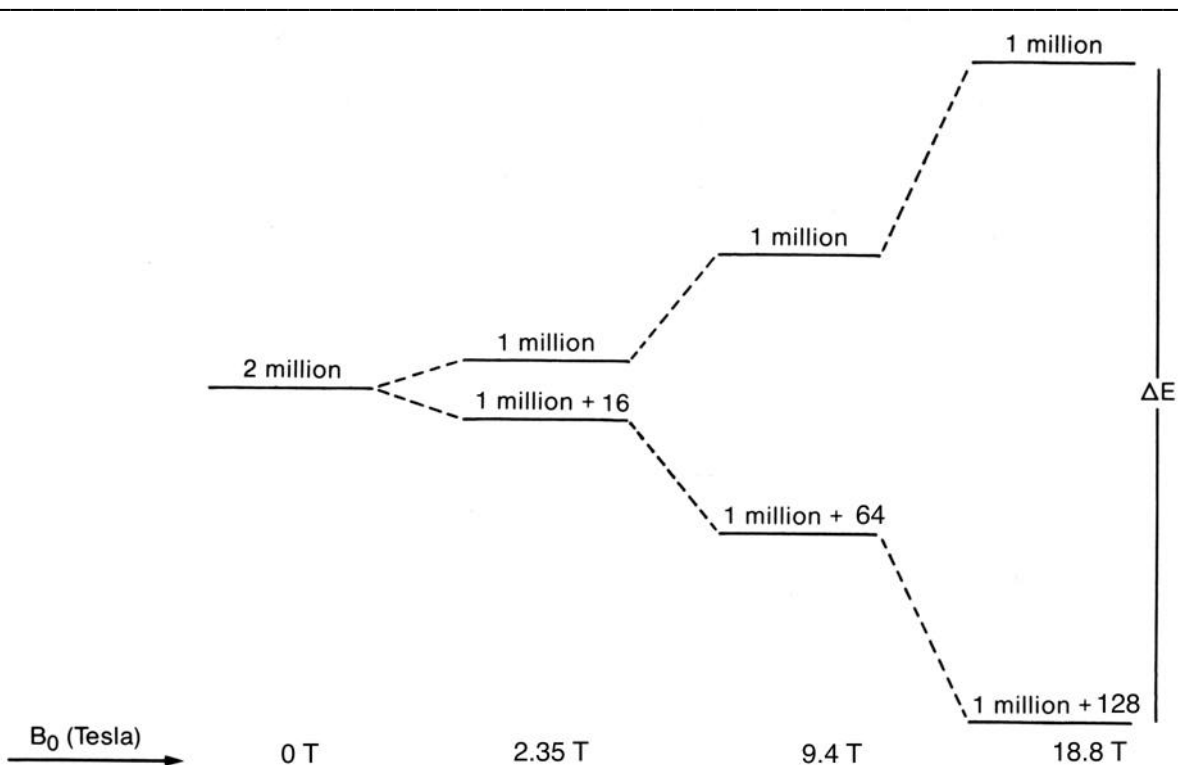
5

Figure 1.3. Dependence on magnetic field strength B_0 of the separation of nuclear energy levels (ΔE) for spin I= 1/2 and the relative populations of the energy levels assuming one has approximately two million protons in the sample (a ridiculously low number in reality).

TABLE 1.1: Properties of Nuclei Most Useful for Biological Studies *

Nucleus	Spin Quantum Number (I)	Natural Abundance (%)	Gyromagnetic Ratio (10^{-7} rad/T sec)	Sensitivity[†] (% vs. ^{1}H)	Electric Quadrupole Moment (Q) (e·10^{24} cm^2)
^{1}H	1/2	99.9844	26.7520	100.0	———————
^{2}H	1	0.0156	4.1067	0.965	0.00277
^{13}C	1/2	1.108	6.7265	1.59	———————
^{15}N	1/2	0.365	-2.7108	0.104	———————
^{19}F	1/2	100	25.167	83.3	———————
^{31}P	1/2	100	10.829	6.63	———————

*From (James, 1975), Appendix 2.

[†]Relative sensitivity for equal number of nuclei at constant magnetic field strength

6

of any RF energy is given by the Boltzmann equation:

$$\frac{N_{upper}}{N_{lower}} = e^{-E/kT} = e^{-h\nu/kT}$$

[1.3]

where N_{upper} and N_{lower} represent the population (i.e., number) of nuclei in upper and lower energy states, respectively, k is the Boltzmann constant, and T is the absolute temperature (˚K). To give some idea of the consequences of increasing magnetic field on the population of spin states, the distribution of a small number (about two million) of hydrogen nuclei, calculated from Equation 1.3, is shown in Figure 1.3. For protons in a 18.8 T magnetic field (ν = 800 MHz) at thermal equilibrium at room temperature, the population ratio will be 0.999872. That means for every 1,000,000 nuclei in the upper energy state there are 1,000,128 nuclei in the lower energy state. Without this small excess number of nuclei in the lower energy state, we would not have NMR.

Such a small population difference presents a significant sensitivity problem for NMR because only the difference in populations (i.e., 128 of 2,000,128 nuclei) is detected; the others effectively cancel one another. The low sensitivity of NMR, which has its origin here, is probably its greatest limitation for applications to biological systems. As seen from Equations 1.2 and 1.3, the use of stronger magnetic fields will increase the population ratio and, consequently, the sensitivity. Different nuclei have different inherent sensitivities; the relative sensitivities are listed in Table 1.1. It should be noted that other factors are also important in detection sensitivity. For example, for macromolecules or small molecules that interact with macromolecules, increasing magnetic field strength often increases relaxation times that can adversely affect sensitivity *(vide infra).*

TABLE 1.2: NMR Sample Size and Concentration for Structural Biology Studies

NMR tube diameter	minimum volume§	¹H (min. conc.)†	Other nuclei (min conc)†
5 mm	0.25 ml	ca. 0.25 mM	ca. 0.5 mM
8 mm	1.0 ml	ca. 0.15 mM	ca. 0.3 mM

§ Exact amount depends on probe and NMR tube design.
† This value can vary significantly depending on NMR instrument sensitivity (magnetic field strength, magnet placement, generation of NMR instrument), linewidths, time willing to spend to collect data, precisely which NMR experiments are being run.

As implied by Equation 1.3, the signal-to-noise (S/N) ratio in an NMR experiment will be enhanced as the number of nuclei in the lower energy state relative to the upper energy state increases. In addition to increasing magnetic field strength, this can be achieved by increasing the number of nuclei in the sample, *e.g.*, by raising the concentration (without causing molecular aggregation) or by increasing the volume of the sample detected. For most types of experiments, the magnetic field strength should be uniform across the sample; to the extent that it is not, the different nuclei in a sample will achieve the Larmor condition (Equation 1.2) at different frequencies leading to a broader signal in the NMR spectrum with a lower S/N ratio. The geometry of the receiver coil used in detecting the NMR signal also has an effect. For biological samples, the high dielectric constant leads to additional signal loss. Table 1.2 gives very approximately the amount and concentration needed for structural studies on nucleic acids, polysaccharides and proteins in the size range 3-25 kilodaltons.

1.2.4 Magnetization

The above description of nuclear magnetization is based essentially on quantum mechanics. However, another way of viewing the NMR phenomenon is to use a classical mechanical description (Abragam, 1961; Ernst et al., 1987). For a spin I = 1/2 nucleus in a magnetic field of strength B_o, the nucleus' magnetic moment will precess about the z-axis defined by the direction of the magnetic field. The angular frequency of precession is $\omega_o = 2\pi\nu_o$, where ν_o is the same linear frequency as used in Equation 1.2, so $\omega_o = \gamma B_o$. In a real sample, we will have a tremendous number of nuclear spins all precessing about the z-axis. This is shown in Figure 1.4 but with a much more tractable number of nuclear spins (arrows). From this discussion, we know that the nuclei may be oriented either parallel or antiparallel to the direction of the magnetic field. Consequently, some spins precess about the positive z-axis and some about the negative z-axis. The magnetization emanating from a real sample is simply the sum of all the individual nuclear magnetic moments (spins). As we know from the previous discussion, there will be a slight excess of nuclei oriented with the magnetic field, i.e., in the lower energy state, so the sum will yield a magnetization (M_o in Figure 1.4) along the positive z-axis. It will be the total magnetization that determines an NMR signal – not the magnetic moment of an individual nucleus.
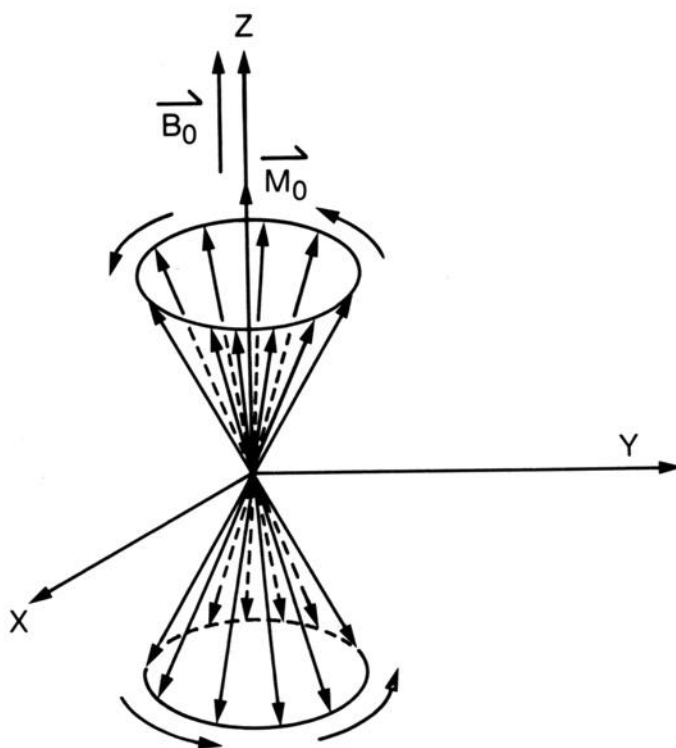
8

Figure 1.4: Orientation and precession of nuclear spins (I = 1/2) at thermal equilibrium in a stationary magnetic field B_O that defines the z-axis. In reality, the angle between the vectors and the z-axis is much smaller than is shown for illustrative purposes. The arrows over $\vec{M}_o$ and $\vec{B}_o$ signify that they are vectors, i.e., that they have direction as well as magnitude.

1.3 The Nuclear Magnetic Resonance Experiment

It is possible to generate a proton NMR spectrum by slowly sweeping either the magnetic field or frequency such that the resonance condition expressed by Equation 1.2 is achieved by all the protons, with signals in the sample occurring successively depending on chemical environment. This method is used for special purposes. However, most spectrometers utilize pulses of radiation which cover the frequency range for all nuclei of a given type, *e.g.*, ^{13}C.

1.3.1 Pulsed Nuclear Magnetic Resonance

The signal-to-noise ratio (S/N) of an NMR signal is dramatically improved by signal averaging, the S/N improving as $\sqrt{n}$, where n is the number of signals averaged. The fastest way to obtain an

NMR signal is to detect the signal following a strong RF pulse applied at the resonance frequency; this signal is the FID. This FID can be followed quickly by another pulse and FID. The second and subsequent FID signals can be acquired by a computer and averaged with the first FID to enhance the S/N. Limitations on the rate of pulsing are set by the acceptable linewidth $W_{1/2}$ for the signal ($W_{1/2}$ pulse repetition rate) and nuclear spinlattice relaxation time T_1 *(vide infra)*: the pulse repetition rate should be less than $1/(4T_1)$ to compare peak areas quantitatively. However, in practice the pulse repetition rate is rarely set so long.

We will now consider how an observable FID can be produced with the aid of Figure 1.5. A rotating coordinate system (x', y', and z) is used in which the x'- and y'-axes are rotating about the z-axis at the NMR instrument's operating frequency (= $_o$). The use of such a coordinate system enables us to consider the effect of applying an RF pulse $\vec{B}_1$, along the x'-axis and observing magnetization (and therefore a signal) along the y'-axis, instead of being concerned about the frequency of the $\vec{B}_1$ pulse and about observation. Figure 1.5A shows the magnetization $\vec{M}_o$ at thermal equilibrium in magnetic field $\vec{B}_o$.
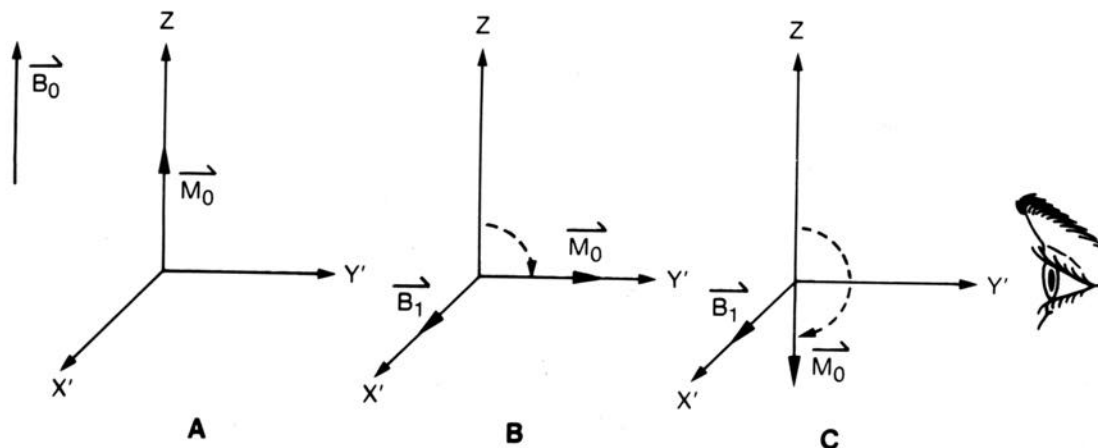

Figure 1.5: Rotation of the magnetization $\vec{M}_o$ in the rotating coordinate system that rotates about the z-axis at the NMR instrument's operating frequency. (A) spin system at equilibrium in magnetic field $\vec{B}_o$; (B) application of a 90° (or /2) $\vec{B}_1$ pulse; and (C) application of a 180° (or) $\vec{B}_1$ pulse.

Magnetization will be rotated in a plane perpendicular to the applied $\vec{B}_1$ pulse, i.e., y'z plane when $\vec{B}_1$ is along x'; of course, the RF pulse $\vec{B}_1$ must be at the appropriate frequency $_o$ as expressed by Equation. 1.2. The angle of rotation depends on the gyromagnetic ratio of the nucleus, the amplitude B_1 of the RF pulse, and the length of time t_w the RF pulse is applied:

10

$$= \text{B}_1 \qquad\qquad\qquad [1.4]$$

Figure 1.5B illustrates the rotation of $\vec{M}_o$ by application of the RF pulse for sufficient time to rotate $\vec{M}_o$ by 90° ($ = $ /2 radians). That pulse is called a 90° or /2 pulse. Application of the $\vec{B}_1$ field for twice as long ($ = $ radians) will result in inversion of $\vec{M}_o$ as shown in Figure 1.5C.

The quantum mechanical analogs of the 90° and 180° pulses of Figure 1.5 are illustrated in Figure 1.6 using our previous examples of two million protons in a 14.1 T magnetic field. The 90° pulse produces an equalization of populations in the two energy states, and the 180° pulse produces an inversion of populations so that the high energy state has a larger number of nuclear spins.
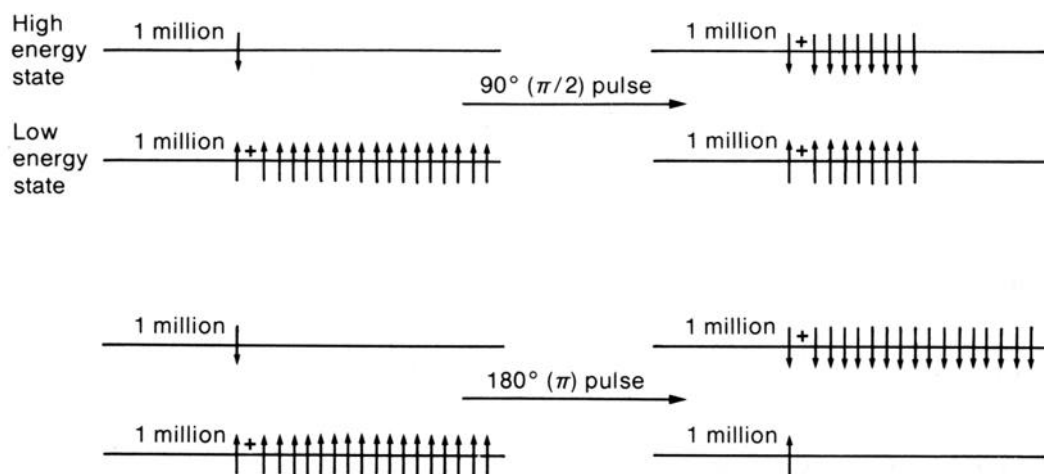

Figure 1.6: Effect of 90° and 180° radiofrequency pulses on the population of nuclear spins in a sample of about two million protons in a magnetic field $\vec{B}_o = 2.35$ T.

1.3.2 Fourier Transform Nuclear Magnetic Resonance

The above discussion on pulsed NMR is sufficient if there is only one frequency for the nuclei of interest, e.g., monitoring the single ^{19}F signal from fluorouracil bound to thymidylate synthase or the proton signal of H_2O in a tissue (because it is present in great excess over other observable proton signals). However, the FID is a time-domain signal with contributions typically from many different nuclei, say the various ^{15}N nuclei in a protein. The usual frequency-domain spectrum can be obtained by computing the Fourier transform of the signal-averaged FID. The signal-averaged

FIDs on the left side of Figure 1.7 yield the frequency spectra on the right side after Fourier transformation.
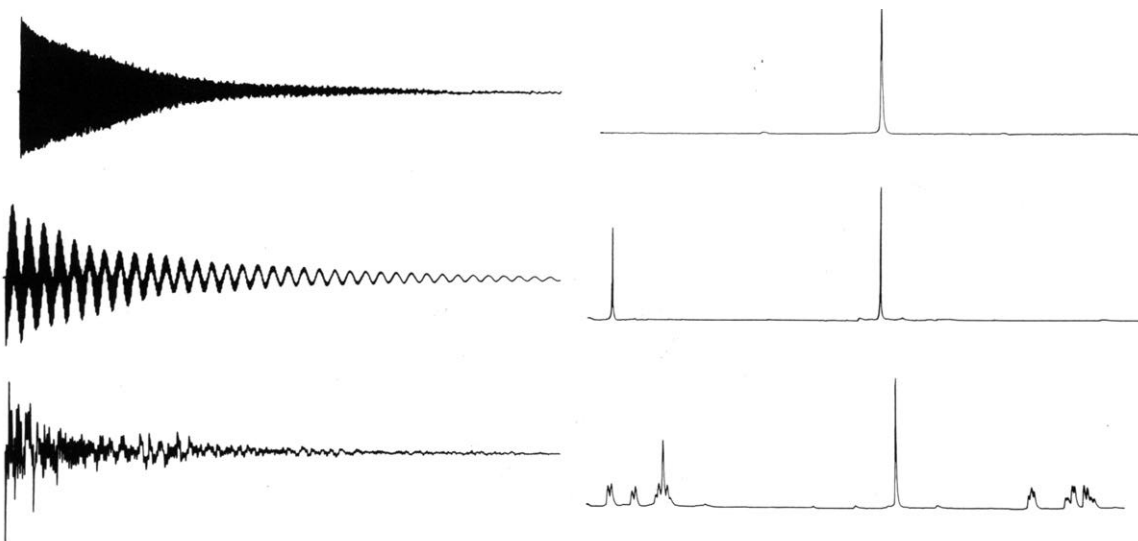
_____

Figure 1.7. The free induction decay (FID) is on the left and its Fourier transform (usual frequency spectrum) is on the right.

_____

1.4   Relaxation

1.4.1 Basis

   We already alluded to relaxation in Figure 1.2 as the process by which a nuclear spin system returns to thermal equilibrium after absorption of RF energy. We can consider any of the spin systems in Figure 1.3 as a starting point. For example, for protons in a 18.8 T field, there will be an excess of 128 of two million in the lower energy state at thermal equilibrium. If RF energy is applied to the nuclear spin system at the resonance frequency *(cf.* Equation. 1.2), the probability of an upward transition is equal to that of a downward transition. Because there is a greater number of nuclei in the lower energy state, there will be more transitions from the lower energy state to the upper state than *vice versa* resulting in a nonequilibrium distribution of nuclear spins. For the protons in the example, the difference will be reduced to <128, even to 0, at which point the NMR signal disappears and the system is "saturated."

12

Relaxation processes, which neither emit nor absorb radiation, permit the nuclear spin system to redistribute the population of nuclear spins. Some of these processes lead to the nonequilibrium spin distribution ($N_{lower} - N_{upper}$) exponentially approaching the equilibrium distribution ($N_{lower} - N_{upper}$)$_{equil}$:
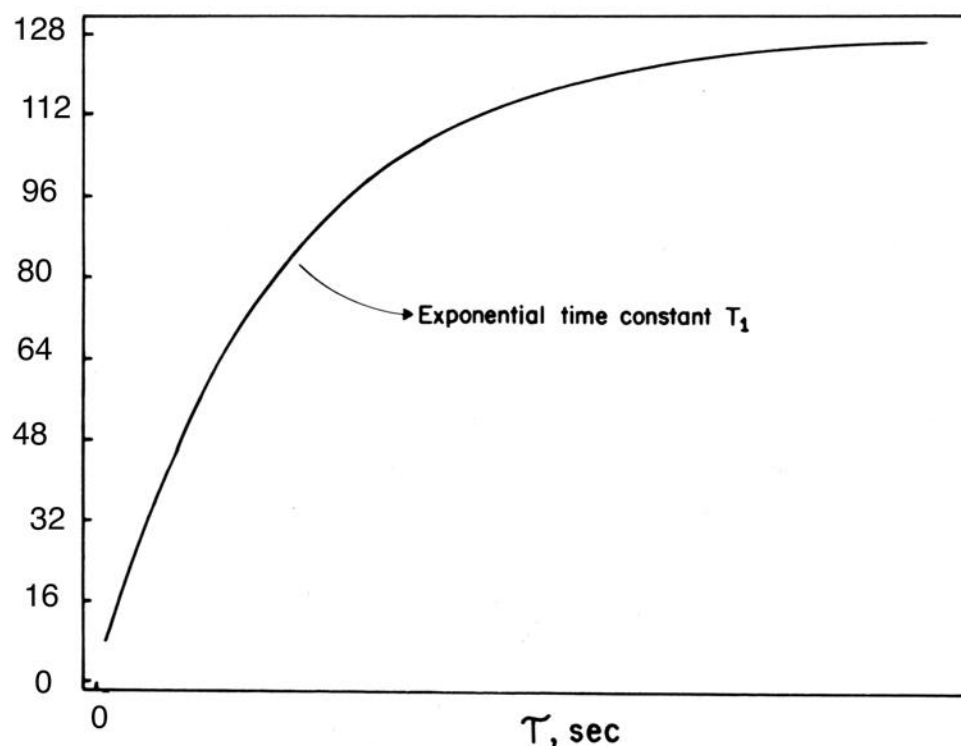

Figure 1.8. Spin-lattice relaxation of a group of 2,000,128 hydrogen nuclei in a magnetic field of strength 18.8 T after saturation of the spin system. The time constant is T_1 for the exponential relaxation of the spin system toward the value of 128, the population difference for that group of nuclei at thermal equilibrium.

$$(N_{lower} - N_{upper}) = (N_{lower} - N_{upper})_{equil} (1 - e^{-\tau/T_1})$$ [1.5

where the time constant for the exponential relaxation is T_1, the spin-lattice relaxation time. Such a relaxation curve is illustrated in Figure 1.8 for the example used above. T_1 is the length of time required for the perturbed system to return 63% of the way toward thermal equilibrium. The lattice is the environment around the nucleus, including other molecules in the sample as well as the remainder of the molecule containing the nucleus of interest. Obviously, different ^{13}C nuclei within the same molecule could have different rates of relaxation, i.e., different T_1 values.

13

There are additional relaxation processes that adiabatically redistribute any absorbed energy among the many nuclei in a particular spin system without the spin system as a whole losing energy. Therefore, the lifetime for any particular nucleus in the higher energy state may be decreased, but the total number of nuclei in that state will be unchanged. This also occurs exponentially and has a time constant T_2, the spin-spin relaxation time. Under some circumstances, the linewidth of an NMR signal at half-height, $W_{1/2}$, can be related to T_2 by

$$W_{1/2} = 1/(\; T_2) \qquad\qquad [1.6]$$

However, in samples containing macromolecules, other factors contribute to make the NMR signal broader than T_2 processes would.

The meaning of T_1 and T_2 may be appreciated by the analogy depicted in Figure 1.9. Energy in the form of heat from the stove is put into the system (house). Relaxation processes will then tend to return the house to thermal equilibrium with the out-of-doors (i.e., cold). Adiabatic T_2 processes will distribute the energy (heat) throughout the system (house), but T_1 processes will dissipate the energy to the out-of-doors (lattice). The uninsulated house on the left represents the situation with small molecules, i.e., $I/T_1 = I/T_2$. The house on the right is insulated so that $l/T_2 > I/T_1$ and consequently represents macromolecular systems *(vice infra)*. (Warning: do not try to push the analogy any further!) Sometimes T_1 is called the *longitudinal relaxation time* because it is a measure of how fast the magnetization relaxes back along the z-axis in Figures 1.4 and 1.5. Likewise, T_2 may be called the *transverse relaxation time* because it measures how fast the spins exchange energy in the transverse (xy) plane of Figures 1.4 and 1.5.
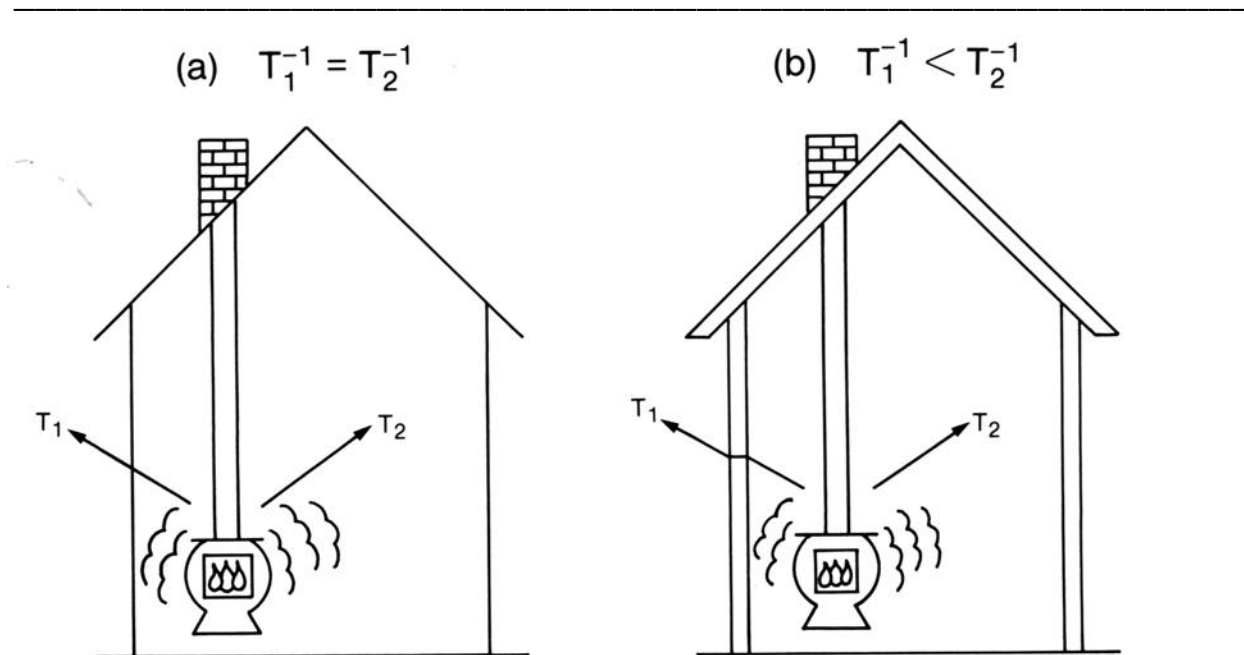
(a) $T_1^{-1} = T_2^{-1}$ **(b)** $T_1^{-1} < T_2^{-1}$

Figure 1.9. Stove-in-a-house analogy to T_1 and T_2 relaxation. In (a), the house is not insulated. so the energy emitted by the stove is lost to the surrounding environment (lattice) as fast as it is dispersed throughout the house. In (b), the house is insulated so that the energy from the stove is not dissipated to the surroundings nearly as fast as it equilibrates in the house.

1.4.2 Causes

For spin-1/2 nuclei, the relaxation processes occur by interaction of the nuclear spin with magnetic fields, produced by magnetic dipoles (e.g., other nuclei, paramagnetic ions), which are fluctuating due to random molecular motions, both rotational and translational (Figure 1.10). The nature and the rate of the molecular motions affect the T_1 and T_2 relaxation times. Molecular motions that occur at a rate comparable to the resonance frequency $_o$ for the nucleus are most effective in promoting spin-lattice relaxation, i.e., yield the lowest values for T_1. T_2 values can be decreased even further as the molecular motion becomes slower than $_o$, but T_1 values will begin to increase. These relationships can be expressed generally as follows:

$$\frac{1}{T_1} = \,^2\overline{H^2}\frac{_c}{1 + (2\,_o\,_c)^2}$$
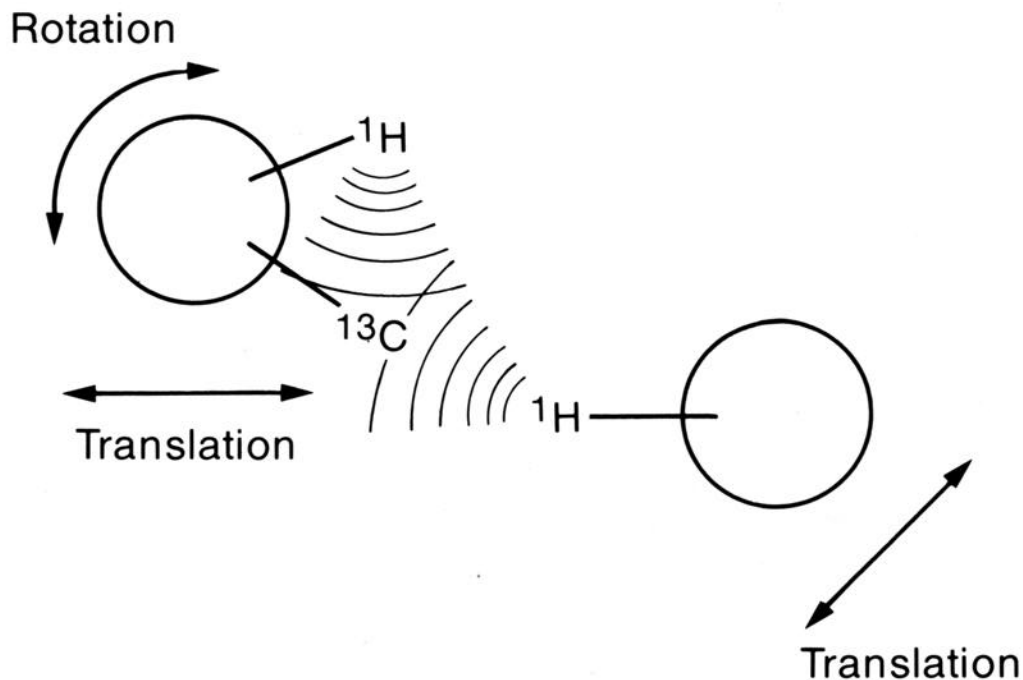
[1.7]

15

Figure 1.10. Relaxation of ^{13}C. Magnetic fields produced by the proton magnetic dipoles are felt by the ^{13}C spin. These local magnetic fields are modulated by random Brownian motions, i.e., ordinary thermal motion. For the proton on the same molecule as the ^{13}C, random rotational fluctuations of the molecule will cause the local magnetic field experienced by the ^{13}C to fluctuate, leading to relaxation of the ^{13}C (*intra*molecular relaxation). Random translational motions of the molecules in solution will cause the ^{13}C to experience a fluctuating magnetic field emanating from the proton on a neighboring molecule, thus causing *inter*molecular relaxation of the ^{13}C.

_____

$$\frac{1}{T_2} = 2\overline{H^2}\left(\tau_c + \frac{\tau_c}{1 + (2\pi\nu_o \tau_c)^2} \right)$$

[1.8]

where $\overline{H^2}$ is the mean-square average of the local magnetic fields, i.e., a measure of the strength

of the interaction between the nuclear spin and the fluctuating magnetic fields, and τ_c is the correlation time. The correlation time is a quantitative measure of the rate of a molecular motion. For rotational motion it is essentially the average length of time required to rotate through an angle of 33°. For translational motion, the correlation time is essentially the average time required for a molecule to move through a distance equal to its diameter.

As implied by Equation 1.7, interaction with the small random fluctuating magnetic fields leads to spinlattice relaxation with the most efficient relaxation effected by motions with $\tau_c = 1/(2\pi\nu_o)$. These same random local magnetic fields are also necessary for spin-spin relaxation, but in this

16

case, relaxation becomes more efficient as the motions become slower (τ_c longer), i.e., as the local magnetic fields become more static (*cf.* frequency-independent τ_c term in Equation 1.8).

These characteristics of T_1 and T_2 are shown in Figure 1.11 as log-log plots of Equations 1.7 and 1.8. It is evident that as τ_c becomes larger, i.e., the molecular motion becomes slower, the value of T_2 becomes smaller than T_1. Typically, the correlation time for molecular motion, either rotational or translational, is 10^{-12} to 10^{-11} sec for small molecules (e.g., water or ATP), 10^{-9} to 10^{-6} sec for macromolecules of increasing size (or small molecules bound to macromolecules), and 10^{-6} to 10^{-3} sec for some motions in membranes. A rough rule of thumb in estimating correlation times is that the value of τ_c for aqueous solutions near room temperature is equal to half of the molecular weight in picoseconds (10^{-12} sec), so a protein with molecular weight of 100,000 has a correlation time of about 50 nsec. Clearly from Figure 1.11, we expect T_1 and T_2 to be equal for small molecules and to differ for macromolecules (or small molecules bound to them). Faster internal motions, e.g., ring-flipping in tyrosine and phenylalanine residues in proteins and sugar repuckering in nucleic acids, can exist in a macromolecule or membrane in addition to overall rotational and translational motions that can make the situation more complicated.

The frequency dependence of T_1 and T_2, expressed in Equations 1.7 and 1.8 by terms containing ω_o, implies that T_1 and T_2 may change if the sample is put in a magnet with a different
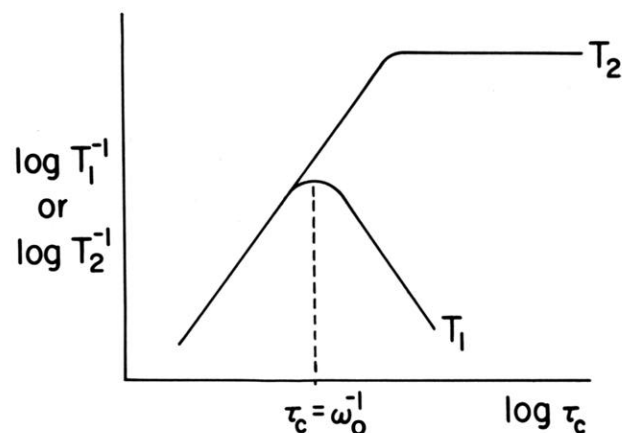

Figure 1.11: Dependence of the relaxation *rates* $1/T_1$ and $1/T_2$ on the rotational correlation time τ_c. τ_c is equal to $2\pi\omega_o$, where ω_o is the spectrometer frequency (*cf.* Equation 1.2). Simple isotropic rotational motion is assumed. T_2 levels off in the rigid lattice limit, i.e., only if the sample is a very cold solid. Clearly, always $T_2 \leq T_1$.

---

field strength B_o (see Equation 1.2 relating B_o to ω_o). Clearly, a larger B_o will lead to a longer T_1 whenever the term $2\pi\omega_o\tau_c$ is comparable to or larger than 1 in Equation 1.7. The value of T_2 may also depend on frequency (and therefore magnetic field strength), but the dependence is

manifest over a smaller range of correlation time values. For extremely small molecules moving freely in solution, and consequently with short τ_c, $2\omega_o$ will be negligible compared with 1 in the denominator of Equation 1.8. For large macromolecules or complexes, τ_c will be large compared to $\tau_c[1+(2\omega_o\tau_c)^2]$, and T_2 will be independent of ω_o (and B_o).

The width of a signal in the NMR spectrum may be related to T_2, as expressed in Equation 1.6. Consequently from the discussion above, we would expect that NMR signals from macromolecules (or ligands bound to them) will be much broader than signals from small molecules free in solution. The increased line broadening is one of the problems in doing NMR studies on ever larger macromolecules. With larger molecules, we will have a greater number of different nuclei increasing the likelihood of signals from the different nuclei being overlapped in a spectrum. As the width of these signals also increases, resolution of the different signals in the spectrum becomes even more difficult. An added detriment is that the amplitudes of the signals decrease as the they broaden, since the peak area of an NMR signal is proportional to the amount of nuclei present. This lower amplitude just exacerbates the signal-to-noise problems of NMR discussed already in the context of the Boltzmann equation.

To illustrate the general concept of relaxation in Figure 1.10, the source of the fluctuating magnetic field interacting with the relaxing ^{13}C was taken to be nearby protons. However, there are other sources of magnetic fields with which the relaxing nucleus can interact in addition to those of magnetic moments of other nuclei, i.e., magnetic moments of unpaired electrons, molecular magnetic moments, and angular variations in the electron shielding of the stationary B_o magnetic field (chemical shift anisotropy). For ^{13}C nuclei the dipole-dipole relaxation mechanism depicted in Figure 1.10 is most important. That mechanism is also dominant for protons and is an important contributor to relaxation of ^{15}N, ^{31}P and ^{19}F. The dipole-dipole mechanism demands that the interacting nuclei be in close physical proximity; indeed, the strength of the interaction diminishes as r^{-6}, where r is the internuclear distance. However, the chemical shift anisotropy (CSA) mechanism is also important for ^{15}N, ^{31}P and ^{19}F. The CSA interaction is the only one requiring the presence of a magnetic field, and it makes a stronger contribution to relaxation as the magnetic field increases.

The magnetic field created by an unpaired electron is much larger than that of a nucleus. In fact, an unpaired electron is half a million times more effective in promoting relaxation than a proton at the same distance from a relaxing nucleus. This is the essential basis for development of paramagnetic contrast agents in NMR. There are other cases of indigenous compounds with

18

unpaired electrons that occur *in vivo*. See Chapters 9 and 10 for a discussion of the mechanism and uses of NMR relaxation effected by unpaired electrons.

Some nuclei possess a spin quantum number I > 1/2 *(e.g.,* ^{2}H and ^{23}Na). These nuclei have a nonspherical nuclear charge distribution and therefore possess an electric quadrupole moment. The interaction of the quadrupole moment with fluctuating electric field gradients around the nucleus provides an efficient relaxation mechanism for these nuclei which usually dominates any other relaxation contribution. Rotational motion is also the relevant motion modulating the interaction.

The relaxation *rate* for a nucleus is the sum of contributions from all mechanisms:

$$\frac{1}{T_1} = \sum_{sources}^{all} \left(\frac{1}{T_1}\right)_i$$

[1.9]

A similar equation could be written for $1/T_2$. Note that the *rates* are additive, not the relaxation times. In general, one or sometimes two mechanisms will dominate the others. A more thorough discussion of relaxation mechanisms may be found in Chapter 8.

1.4.3 Measurement

Several different pulse sequences have been utilized to measure T_1 and T_2. The most common (and probably best) technique for determining T_1 is to employ the inversion recovery sequence ($180° - \tau - 90°$). After an initial $180°$ pulse inverts the spin populations *(cf.* Figure 1.5), the spin system begins relaxing toward thermal equilibrium as discussed earlier. After time τ, a $90°$ pulse is applied, and the FID following the pulse is acquired. As τ becomes longer, the magnetization more closely approaches the equilibrium population distribution of Figure 1.5A rather than the inverted magnetization of Figure 1.5B. A $90°$ pulse must be applied to be able to detect any magnetization because detection is possible only in the transverse plane (see eye in Figure 1.5). The value of T_1 may be determined by measuring the magnitude M of the FID as a function of τ using the following expression:

$$M = M_\infty (1 - 2e^{-\tau/T_1})$$

[1.10]

where M_∞ is the magnitude of the FID when τ = infinity (i.e., at thermal equilibrium).

Determination of T_2 is best carried out using a CarrPurcell pulse sequence with the Meiboom-Gill modification. Figure 1.12 illustrates the process in the rotating coordinate frame. An initial

19

90° pulse rotates the magnetization into the y' direction. Because the B_o magnetic field is not perfectly homogeneous, the individual magnetic spins will have slightly different precessional frequencies (*cf.* Equation 1.2). Consequently, the individual spins will fan out in the xy' plane with a loss of *phase coherence* (C). After a time , a 180° pulse is applied (D). Because
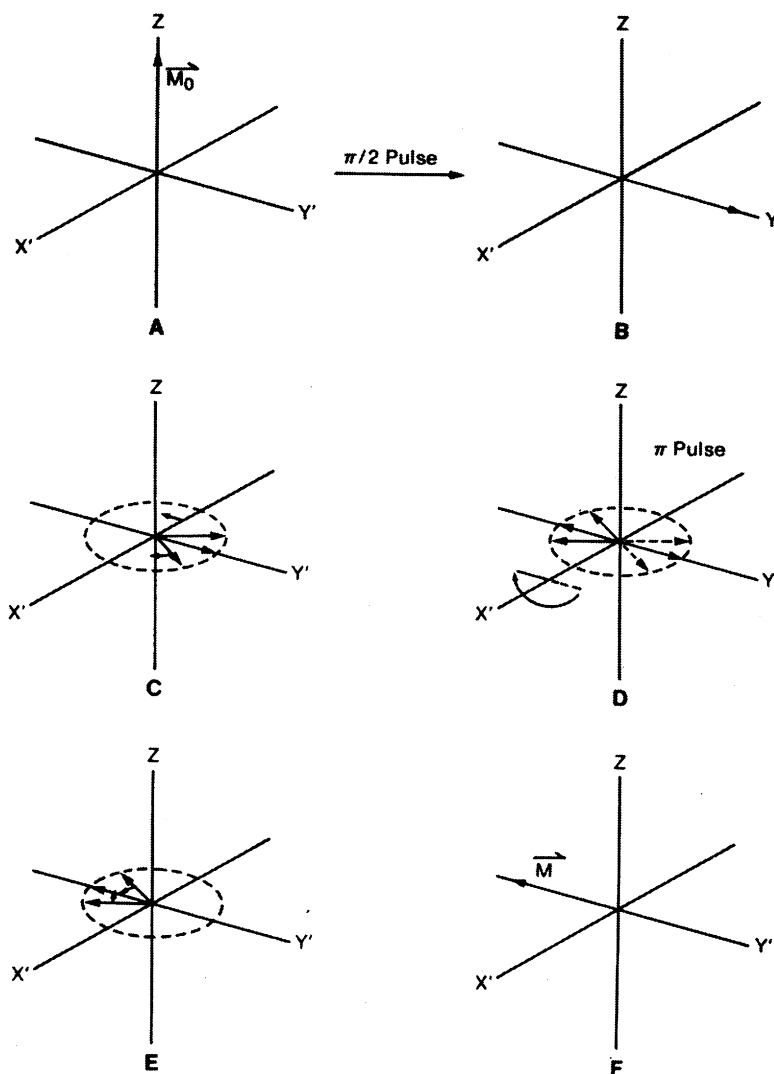

Figure 1.12: The 90°- -180° T_2 experiment. Radiofrequency pulses of strength B_1 are applied along the x'-axis in the rotating coordinate system. Detection is along the y'-axis so a signal can be detected after the 90° pulse (B) and at formation of the spin-echo (F).

the precessional frequencies of the individual spins are unchanged (E), they will then achieve phase coherence at time 2 along the negative y' axis (F). This will result in a signal, called a *spin-echo,* being detected. Following the spin-echo, phase coherence will again be lost but can be regained with another 180° pulse. The Carr-Purcell sequence is initiated with a 90° pulse followed

20

by a series of 180° pulses. The result is a train of spin-echoes, signals that follow each 180° pulse exactly halfway between the 180° pulses. The magnitudes of the echoes decay exponentially as the train of echoes progresses, so that the echo magnitude can be expressed as

$$M = M \quad e^{-t/T2} \qquad\qquad [1.11]$$

where t is the length of time from the 90° pulse to the top of an echo. Obviously, T_2 can be determined from the decay of the echo amplitudes. For T_1 and T_2 determination of individual signals in an NMR spectrum, the peak amplitudes are monitored as a function of interpulse spacing
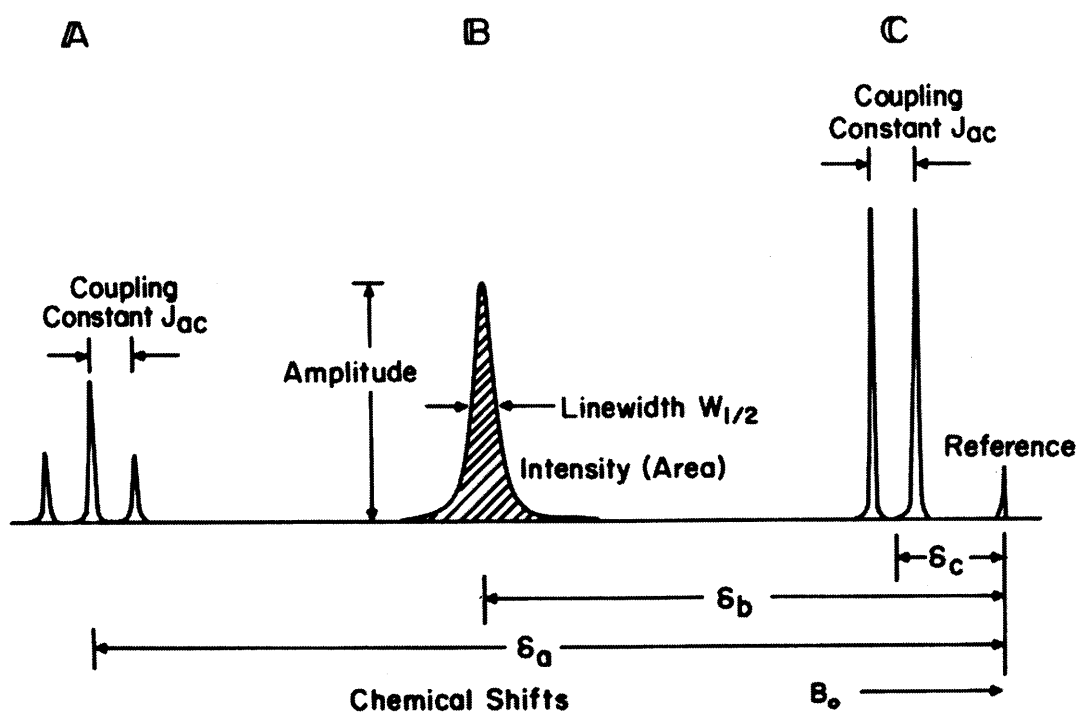
.

_____

Figure 1.13: Nuclear magnetic resonance spectral parameters.

_____

1.5 Other Nuclear Magnetic Resonance Parameters

1.5.1 General Features of Nuclear Magnetic Resonance Spectrum

   The various NMR spectral parameters to be discussed subsequently are illustrated in Figure 1.13. Clearly, a one-dimensional spectrum is represented. However, as we encounter two-, three-

21

or four-dimensional spectra, it should be apparent how the features mentioned here may be manifest in those multidimensional spectra.

1.5.2 Chemical Shift

It is obvious from Equation 1.2 that nuclei of different elements, having different gyromagnetic ratios, will yield signals at different frequencies in a particular magnetic field. However, it also turns out that nuclei of the same type can achieve the resonance condition at different frequencies. This can occur if the local magnetic field experienced by a nucleus is slightly different from that of another similar nucleus; for example, the two ^{13}C NMR signals of ethanol occur at different frequencies because the local field that each carbon experiences is different.

The reason for the variation in local magnetic fields can be understood from Figure 1.14. If a molecule containing the nucleus of interest is put in a magnetic field B_o, simple electromagnetic theory indicates that the B_o field will induce electron currents in the molecule in the plane perpendicular to the applied magnetic field. These induced currents will then produce a small magnetic field opposed to the applied field that acts to partially cancel the applied field, thus shielding the nucleus. In general, the induced opposing field is about a million times smaller than the applied field. Consequently, the magnetic field perceived by the nucleus will be very slightly altered from the applied field, so the resonance condition of Equation 1.2 will need to be modified:

$$= (\ /2 \ )B_{local} = (\quad /2 \ )(1- \ ) \hspace{3cm} [1.12]$$

where B_{local} is the local field experienced by the nucleus and   is a nondimensional screening or *shielding constant*. The frequency   at which a particular nucleus achieves resonance clearly depends on the shielding which reflects the electronic environment of the nucleus.
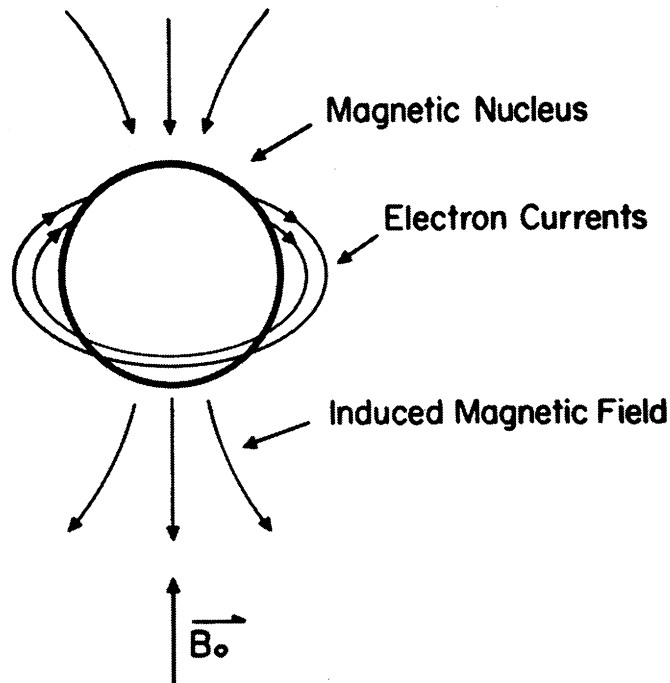
22

Figure 1.14: Electron currents around a nucleus are induced by placing the molecule in a magnetic field B_o. These electron currents, in turn, induce a much smaller magnetic field opposed to the applied magnetic field B_o.

There will be more electronic currents induced in the molecule than just those directly around the nucleus. In fact, some of those currents may increase B_{local} (*cf.* Figure 1.15). Therefore, the shielding and the resulting resonance frequency will depend on the exact characteristics of the electronic environment around the nucleus. The induced magnetic fields are typically a million times smaller than the applied magnetic field. So if the Larmor resonance frequency $_o$ is on the order of several megahertz, differences in resonance frequencies for two different hydrogen nuclei, for example, will be on the order of several hertz. Although we cannot easily determine absolute radiofrequencies to an accuracy of ±1 Hz, we can determine the relative positions of two signals in the NMR spectrum with even greater accuracy. Consequently, a reference signal is chosen, and the difference between the position of the signal of interest and that of the reference is termed the *chemical shift.*.

Although a chemical shift could be expressed as the frequency difference in hertz, it is clear from either Equation 1.2 or 1.12 that the chemical shift in Hz would depend on the magnetic field in which the sample was placed. To remove the dependence of the chemical shift on magnetic field
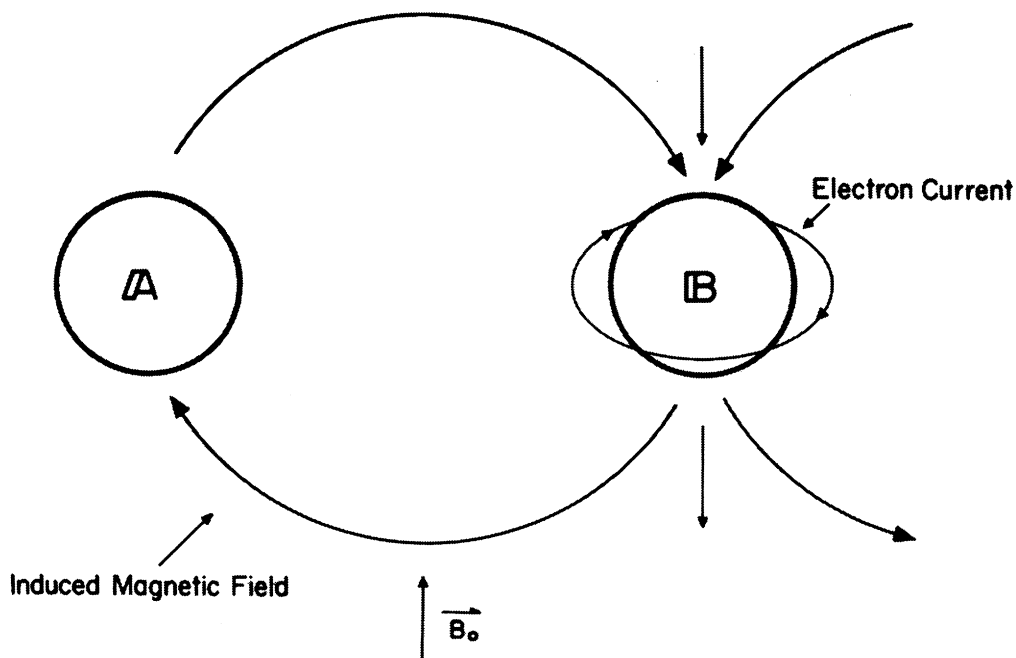
23

Figure 1.15: Effects at nucleus X caused by the secondary magnetic field arising from induced electronic currents at nucleus Y.

___

strength and therefore operating frequency, the chemical shift is usually expressed in terms of parts per million (ppm), actually a dimensionless number, by

$$= \frac{\text{ref} - \text{sample}}{\text{sample}} \times 10^6$$

[1.13]

where the difference between the resonance frequency of the reference and the sample ($_{\text{ref}}$ - $_{\text{sample}}$) measured in hertz (e.g., 75 Hz) divided by the spectrometer's operating frequency (e.g., 500 MHz) gives the chemical shift (e.g., 0.15 ppm). Typical ranges in chemical shifts for signals emanating from biochemically important samples are ^{1}H, 15 ppm; ^{13}C, 250 ppm; ^{15}N, 400 ppm; and ^{31}P, 35 ppm.

1.5.3 Spin-Spin Coupling (Splitting)

A nucleus with a magnetic moment may interact with other nuclear spins resulting in mutual splitting of the NMR signal from each nucleus into multiplets. The number of components into

24

which a signal is split is 2nI+1, where I is the spin quantum number *(cf.* Table I) and n is the number of other nuclei interacting with the nucleus. For example, a nucleus (e.g., ^{13}C or ^{1}H) interacting with three methyl protons will give rise to a quartet. To a first approximation, the relative intensities of the multiplets are given by binomial coefficients: 1:1 for a doublet, 1:2:1 for a triplet, and 1:3:3:1 for a quartet. The difference between any two adjacent components of a multiplet is the same and yields the value of the spin-spin coupling constant J (in hertz).

One important feature of spin-spin splitting is that it is independent of magnetic field strength. So increasing the magnetic field strength will increase the chemical shift difference between two peaks in hertz (not parts per million), but the coupling constant J will not change.

To simplify a spectrum and to improve the S/N ratio, *decoupling* (usually of protons) is often employed, especially with ^{13}C and ^{15}N NMR. Strong irradiation of the protons at their resonance frequency will cause a collapse of the multiplet in the ^{13}C or ^{15}N resonance into a singlet.

1.5.4 Linewidth

The relationship between the minimum linewidth $W_{1/2}$ and T_2 relaxation has already been given in Equation 1.6. In samples with macromolecules the linewidth may be broader than the scalar splitting, so the latter may not necessarily be apparent. It should also be noted that rapidly exchanging –OH and –NH protons *(vide infra)* do not cause splitting. However, if coupling constants can be determined, they can sometimes reveal details about molecular geometry.

1.5.5 Peak intensity

The area of an NMR signal (the peak intensity), but *not* the height (the peak amplitude), is directly proportional to the number of nuclei contributing to the signal under suitable experimental conditions. Those conditions are that the delay between acquiring free induction decays for signal averaging purposes should be $\approx 4T_1$ *(vide supra).* Consequently, if the concentration of nuclei is known for a particular peak, it can be used as a standard. This delay is required for complete relaxation (well, nearly — see equation 1.10) of *all* nuclei. As already noted, to achieve the best S/N for a given time of signal acquisition, spectroscopists typically do not wait for full relaxation. For some types of NMR experiments, a comparison of peak intensities is required (e.g., for nuclear Overhauser effect measurements — see Chapter 5). The practitioner should recognize that the different peak intensities may not be compared rigorously but approximately when the pulse delay is not sufficient for full relaxation.

25

1.6 Nuclear Overhauser Effect (NOE)

   The nuclear Overhauser effect or NOE is a relaxation parameter which has been used as the primary tool for determining three-dimensional molecular structure (see Chapter 5, as well as the list of references to this chapter). When two nuclei are in sufficiently close spatial proximity, there may be an interaction between the two dipole moments. The interaction between a nuclear dipole moment and the magnetic field generated by another was already noted to provide a mechanism for relaxation. The nuclear dipole-dipole coupling thus leads to the NOE as well as T_1 relaxation. If there is any mechanism other than from nuclear dipole-dipole interactions leading to relaxation, e.g., from an unpaired electron, the NOE will be diminished – perhaps annihilated.
   While it is possible to measure an NOE from a 1D NMR spectrum, usually 2D NOE (or sometimes 3D NOE) experiments are performed. Figure 1.16 shows the 2D NOE pulse sequence and a schematic 2D NOE spectrum. The intensities of the cross-peaks in the spectrum depend on the distance between the interacting nuclei; it is this relationship that provides structural information. While the situation is actually more complicated 1991 ***15*** as long as the mixing time is kept short (in practice <100 msec), to a first approximation the cross-peak intensity decreases with increasing internuclear distance r according to r^6. The 2D NOE spectrum in Figure 1.16 thus would imply that protons 1 and 2 are in close proximity, 2 and 3 are further apart, while 2 and 4 are separated yet further. With current high field instruments, it is possible to detect cross-peaks from protons up to 5-6 Å apart.(possibly 7 Å if methyl protons are involved); this is applicable to molecules which have a correlation time larger than *ca.* one nanosecond.
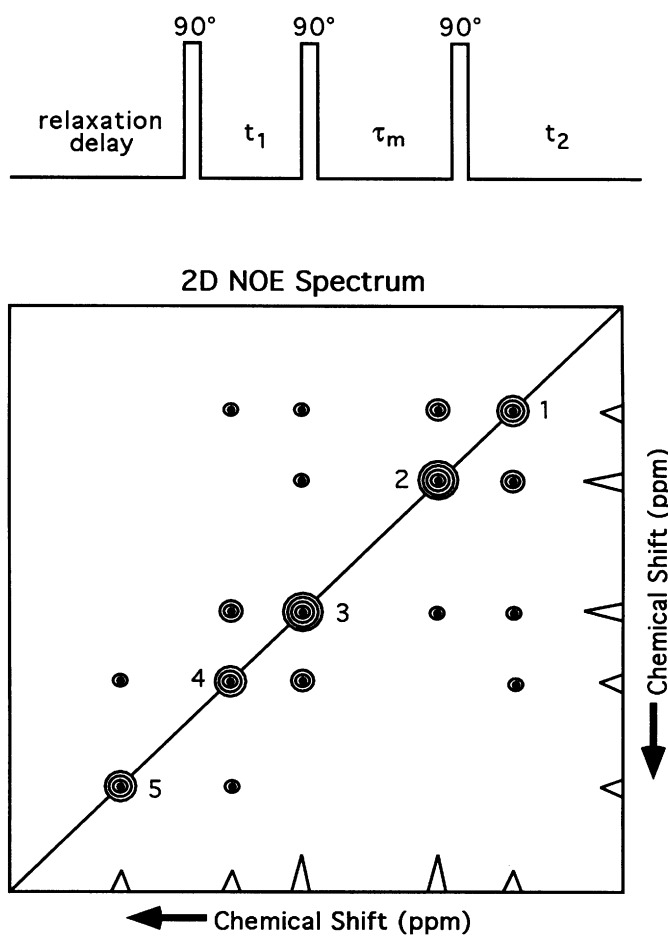
26

Figure 1.16: Basic pulse sequence to obtain a 2D NOE spectrum (top). For simplicity, we can assume that we are dealing only with protons. The relaxation delay simply denotes the time period to allow for nuclear relaxation before application of the pulse sequence for signal averaging purposes as discussed in section 1.5.5. As shown in Figure 1.12, the initial 90° pulse rotates the magnetization into the x'y' plane. The spins of nuclei with different chemical shifts have different precessional frequencies (*vide supra*), so after time t_1 the extent of magnetization in the x'y' plane (sum up all individual nuclear spin vectors) for nuclei with different chemical shifts will differ. The second 90° pulse rotates the transverse magnetization onto the z-axis and during the mixing time period, cross-relaxation can occur. The effect of cross-relaxation during the mixing time is to transfer magnetization between neighboring protons. The third 90° pulse rotates the magnetization again into the x'y' where it can be detected during the acquisition time t_2. Fourier transformation (FT) of the free induction decay acquired during t_2 yields a 1D spectrum which will depend upon the length of the mixing time $_m$ and the value of t_1. The acquisition and Fourier transformation can

27

be repeated several times with incrementally varying values of t_1. The intensity of any signals in the resulting 1D spectra will be modulated at a frequency depending upon chemical shift. A second Fourier transformation can be carried out as a function of t_1, just as the individual spectra were generated via FT as a function of t_2. The result is a 2D NOE spectrum with frequency axes corresponding to the two separate Fourier transformations. If nuclei which are frequency-labeled according their chemical shifts during t_1 interact with nuclei with a different chemical shift during $_m$, in addition to the peaks along the diagonal, cross-peaks occur in the 2D NOE spectrum corresponding to the two different chemical shifts. This is illustrated schematically in the lower figure for signals from five protons. Note that a projection along either axis yields the same information as the 1D NMR spectrum, but the 2D NOE spectrum gives us the additional data about relative proximity of protons in the molecule.

_____

1.7 Chemical Exchange

The subject of chemical exchange is vital to biological NMR. A detailed discussion of the subject has been presented (Lane and Lefèvre, 1994). Nuclear magnetic resonance parameters can be affected by the monitored nucleus spending part of its time in one environment and part of its time in another environment (and possibly more). If the exchange between the environments is sufficiently rapid, the observed NMR parameter will be a weighted average of the parameter values in each of the different environments or sites, the weighting taking account of the relative number of nuclei in each of the sites. One often-encountered example of exchange is provided by the observation of the ^{1}H NMR of molecules containing hydroxyl, amide or amino groups in aqueous solution (Figure 1.17). Generally, the protons on these functional groups exchange so quickly with H_2O protons that only a single averaged resonance signal is seen for these "exchangeable" protons; because H_2O is usually present in great excess, the properties of this averaged resonance signal are weighted such that bulk H_2O protons dominate. It should be noted, however, that in proteins and nucleic acids, the complicated structure precludes much of that exchange thus enabling signals from these hidden "exchangeable" protons to be observed. Observation of signals from amide protons of proteins, for example, is invaluable for ascertaining parts of the molecule which do or do not become exposed to solvent water. Observation of signals from imino (and sometimes amino) protons in nucleic acids likewise demonstrate stability of base pair formation.

Another example of exchange is that of a small molecule that may spend part of its time free in solution and part bound to a macromolecular structure. It's properties will reflect that averaging as long as the exchange is sufficiently fast (*vide infra*).
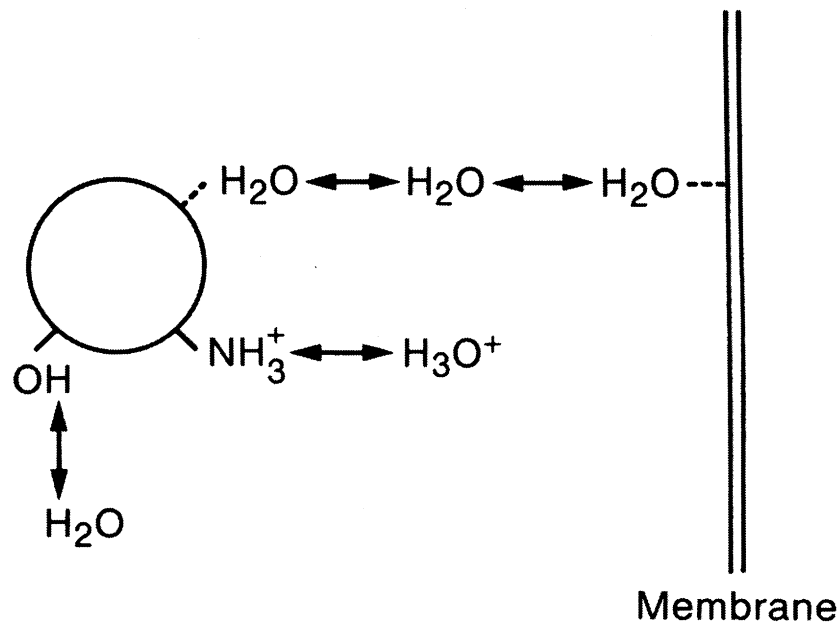
Figure 1.17: Chemical exchange processes. A proton which contributes to the observed H_2O proton resonance signal may spend part of the time free in solution and part of the time bound to membranes and molecules either on the H_2O molecule *per se* or on hydroxyl, $-NH_3^+$, $-COOH$, $-CONH-$, or other OH and NH groups.

With rapid exchange between the two sites A and B, a single resonance signal centered at frequency

$$= f_A \, _A + f_B \, _B \qquad [1.14]$$

with linewidth $W_{1/2}$ [$= 1/(1/T_2)$] such that

$$1/T_2 = 1/T_{2A} + 1/T_{2B} \qquad [1.15]$$

and

$$1/T_1 = 1/T_{1A} + 1/T_{1B} \qquad [1.16]$$

where f_A and f_B represent the fractions of nuclei at sites A and B, and the subscripts A and B refer to the values of those parameters when the rapidly exchanging nuclei are in sites A or B. Of

29

course, $f_A + f_B = 1$. For rapid exchange to occur, the exchange rate must be much larger than (a) the chemical shift difference $\nu_A - \nu_B$, (b) $1/T_{2A} + 1/T_{2B}$, and (c) $1/T_{1A} + 1/T_{1B}$. The other limit is that of *slow exchange* in which case two separate resonance peaks occur in the spectrum for nuclei in sites A and B; the conditions for this are just the opposite of those for rapid exchange. This occasionally occurs when two different conformations of a molecule are energetically comparable and interconversion of the two different conformations is slower than $\nu_A - \nu_B$, i.e., the rate of interconversion is less than ~10^2 sec^{-1}. When exchange rates are on the same order as $\nu_A - \nu_B$, $1/T_2$, or $1/T_1$ the situation is more complicated, with additional line broadening occurring; sometimes the broadening of signals from this intermediate exchange condition is so extreme that the signals can no longer be observed in the spectrum. When either the rapid exchange limit or the slow exchange limit is just slightly violated, the small amount of additional line broadening from the exchange process itself can be used to determine the exchange rate.

It should be realized that all measurable NMR parameters will be averaged by exchange. For rapid exchange, equations analogous to 1.14, 1.15, and 1.16 will pertain.

It can be seen readily from Equations 1.15 and 1.16 that the measured relaxation time values of a small molecule can be affected significantly if that small molecule spends part of its time bound to macromolecular structures and rapid exchange occurs. For example, if only 1% of the rapidly exchanging small molecule is bound to the macromolecule, the linewidth will double if the molecular motion is 100 times slower in the bound state; in practical situations, the molecular motion may be 10^2 to 10^6 times slower.

REFERENCES

Abragam, A. 1961. Principles of Nuclear Magnetism. Oxford University Press, Oxford.

Cavanagh, J., W. J. Fairbrother, A. G. Palmer III, and N. J. Skelton. 1996. Protein NMR Spectroscopy: Principles and Practice. Academic Press, Inc., San Diego.

Derome, A. 1987. Modern NMR Techniques for Chemistry Research. Pergamon Press Press, Oxford.

Ernst, R. R., G. Bodenhausen, and A. Wokaun. 1987. Principles of Nuclear Magnetic Resonance in One and Two Dimensions. Clarendon Press, Oxford.

James, T. L. 1975. Nuclear Magnetic Resonance in Biochemistry. Academic Press, New York.

James, T. L. 1991. Relaxation Matrix Analysis of 2D NOE Spectra to Obtain Accurate Biomolecular Structural Constraints and to Assess Structural Quality. *Curr. Opin. Struct. Biol.* 1:1042-1053.

James, T. L. 1995. Nuclear Magnetic Resonance and Nucleic Acids. Methods in Enzymology. Academic Press, New York. 644.

James, T. L., and N. J. Oppenheimer. 1994. Nuclear Magnetic Resonance, Part C. Methods in Enzymology. Academic Press, New York. 813.

Lane, A. N., and J.-F. Lefèvre. 1994. Nuclear Magnetic Resonance Measurements of Slow Conformational Dynamics in Macromolecules. *Meth. Enzymol.* 239:596-619.

Reid, D. G. 1997. Protein NMR Techniques. Methods in Molecular Biology. Humana Press, Totowa, New Jersey. 419.